PAPER

Check for updates

PoCOsteo: generic novel platform for bone turnover marker measurement & monitoring†

Patricia Khashayar, [ID] *[ab] Paula Lopes,[ai] Peter Ragaert,[c] Richard Hoogenboom, [ID] [d] Daniel Latta,[e] Rainer Gransee,[e] Daniel Lenartowicz,[f] Phil Biggs,[f] Ikerne Etxebarria,[g] Barbara Luegger,[h] Barbara Obermayer-Pietsch,[h] Hans Peter Dimai[h] and Jan Vanfleteren [ID] [a]

Despite the increasing efforts in improving bone health assessments, current diagnostics suffer from critical shortcomings. The present article therefore describes a multiplex label-free immunosensor designed and validated for the assessment of two bone turnover markers (BTMs), namely beta isomerized C-terminal telopeptide of type I collagen (CTx) and Procollagen I Intact N-Terminal (PINP), the combination of which is needed to illustrate an accurate overview of bone health. The immunosensor was then tested outside and inside of a microsystem, with the aim of becoming compatible with a point of care system fabricated for automated assessment of these biomarkers later-on at patient side. Custom-made monoclonal antibodies were specifically designed for this purpose in order to guarantee the selectivity of the immunosensor. In the final platform, a finger prick blood sample is introduced into the microfluidic manifolds without any need for sample preparation step, making the tool suitable for near patient and outside of the central laboratory applications. The platform was exploited in 30 real blood samples with the results validated using electrochemiluminescence immunoassay. The results revealed the platform was capable of measuring the target analyte with high sensitivity and beyond the recommended clinical reference range for each biomarker (CTx: 104–1028 ng L^{-1} and PINP: 16–96 μg L^{-1}, correspondingly). They also showed the platform to have a limit of detection of 15 (ng L^{-1}) and 0.66 (μg L^{-1}), a limit of quantification of 49 (ng L^{-1}) and 2.21 (μg L^{-1}), and an inter- and intra-assay coefficient of variance of 5.39–6.97% and 6.81–5.37%, for CTx and PINP respectively, which is comparable with the gold standard. The main advantage of the platform over the state-of-the art was the capability of providing the results for two markers recommended for assessing bone health within 15 minutes and without the need for skilled personnel or costly infrastructure.

1. Introduction

Osteoporosis is a silent killer, affecting 18.3% of the population worldwide.[1] This is while osteoporosis is largely preventable thanks to the remarkable progress in the scientific understanding of its causes, diagnosis, and treatment.[2] However, the prediction of rapid bone loss along with the incidence of osteoporosis and osteoporotic fracture remains difficult. Dual-energy X-ray absorptiometry (DXA), the current gold standard for osteoporosis diagnosis, can only detect the problem when a large amount of bone is lost and there is no way back other than expensive bone regeneration therapies.[3] This technique also has a low sensitivity for identifying individuals at risk of fracture, with the majority of osteoporotic fractures occurring in those with bone mass values above the osteoporosis threshold.[4] Proteomics and mainly bone turnover markers (BTMs) measurements, determining the activity of bone cells, on the other hand, can provide a better overview of bone loss and response to treatment.[5,6]

Enzyme-linked immunosorbent assay (ELISA) and electrochemiluminescence (ECLIA), the state-of-art technique for BTM measurements requires expensive and elaborate analysis infrastructure, is highly dependent on skilled human/robots, suffers from long sample-to-result lead times and needs large

Center for Microsystems Technology, Imec & Ghent University, Zwijnaarde, Gent, Belgium. E-mail: Patricia.khashayar@ugent.be

[b]International Institute for Biosensing, University of Minnesota, Minneapolis, USA

[c]Research Unit Food Microbiology and Food Preservation, Faculty of Bioscience Engineering, Ghent University, Gent, Belgium

[d]Supramolecular Chemistry Group, Centre of Macromolecular Chemistry, Department of Organic and Macromolecular Chemistry, Ghent University, Ghent 9000, Belgium

[e]Fraunhofer-Institut für Mikrotechnik und Mikrosysteme IMM, Mainz, Germany

[f]Labman Co., Middlesbrough, TS9 5NQ, UK

[g]TE Connectivity, 20500 Arrasate, Gipuzkoa, Spain

[h]Department of Internal Medicine, Division of Endocrinology and Diabetology, Medical University of Graz, Graz, Styria, Austria

[i]International Iberian Nanotechnology Laboratory, Braga, Portugal

† Electronic supplementary information (ESI) available. See DOI: https://doi.org/10.1039/d4ay00207e

sample and reagent volumes. These shortcomings have become increasingly critical in modern societies, as the need for rapid, accurate and low-cost analysis has proven to be more pressing.[7,8] As for osteoporosis, these shortcomings are shown to be linked with low compliance commonly reported in these patients. Not being able to provide the changes in the marker levels in real time coupled with the fact that the patients do not feel any plausible transformations following treatment are reported as the main reasons for many patients having a poor adherence to their treatment.[9]

Lab-on-Chip (LoC) and biosensing technology aims to overcome these restrictions, through integration of one or several analyses onto a single miniaturized chip in order to provide test results in real time.[10,11] Other advantages include cost efficiency, parallelization, portability, diagnostic speed, and sensitivity. Several studies have pointed out the fact that having the results in real time and during the consultation time can help improve the patients' compliance with treatment.[12]

Multiple attempts have been made in the previous years to fabricate biosensors suitable for measuring different BTMs.[13–20] As explained in the review by Khashayar et al., most of these biosensors have been designed for a single biomarker (mainly beta isomerized C-terminal telopeptide of type I collagen (CTx) or osteocalcin (Oc)).[21] This is while the International Osteoporosis Foundation (IOF) recommends the combination of a bone formation (Procollagen I Intact N-Terminal (PINP)) and a resorption (CTx) marker as the most efficient combination in diagnosing high turnover individuals at risk of osteoporosis and for monitoring the treatment process.[22,23] CTx is a bone resorption marker with a broad dynamic range (130–1700 ng L^{-1}, depending on age and gender according to the MayoClinic Test catalogue), the high levels of which are linked with a pathologic condition associated with high bone turnover.[24] This is while PINP is a bone formation marker with a reference range of 16–96 µg L^{-1} (depending on gender according to the MayoClinic Test catalogue) and its low concentrations signify insufficient bone production and various bone conditions.[25] These characteristics call for a diagnostic capable of measuring both low and high values accurately to allow precise patient identification and treatment monitoring. Combining the two markers on a single platform, therefore, could be challenging and to our knowledge no such a biosensor exists. The only currently existing multiplex automated assays specific for osteoporosis are developed by Roche and IDS iSYS; they however need expensive infrastructures and thus their use is limited to specific central labs. They are therefore not accessible for everyone nor are they suitable for in-office or real time testing.[26] In previous projects, we successfully developed a proteomic electrochemical immunosensor capable of detecting serum levels of different BTMs.[27] The performance of the proof-of-concept sensor was highly correlated with that of the ECLIA assays, as the state-of-the-art. While its dynamic range was within the acceptable reference range for the CTx and Oc, a broader dynamic range was needed for the application. Moreover the short shelf-life of the immunosensor as well as their long fabrication time made them not suitable for mass manufacturing.

In this regard OsteoLab is designed in the context of PoCOsteo, a Horizon 2020 project to develop a point of care diagnostic (appropriate for in-office use), for accurate (compared with state-of-the-art), robust, and reproducible measurement of BTMs, namely CTx and PINP, within a broad reference range (compatible both for the screening and monitoring purposes) in real time and with a minimum shelf-life of 6 months.

2. Materials and methods

2.1. Material

Custom-made high-temperature screen-printed gold electrodes were purchased from C-Mac, Belgium. Casein, 1-octadecanethiol (ODT), phosphate buffered saline (PBS), PBS-Tween 20, and potassium hexacyanoferrate(III) (K$_3$ [Fe(CN)$_6$]) and potassium hexacyanoferrate(II) (K$_4$ [Fe(CN)$_6$]) were purchased from Sigma-Aldrich (Diegem, Belgium). Custom-made monoclonal CTx antibody and protein (beta isomerized CTx) as well as PINP antibody and protein (intact molecule) were developed by Proteogenix (France). The two proteins are called the analytes throughout the article.

2.2. Equipment

Electrochemical studies, namely cyclic voltammetry and Differential Pulse Voltammetry (DPV) were utilized to characterize the electrochemical behavior and performance of the electrode arrays. Cyclic voltammetry measurements were run in the potential window from −0.30 V to +0.4 V at a scan rate of 0.05 V s^{-1} using two subsequent scans. DPV was performed using following parameters, 0.025 V modulation amplitude, 0.025 s modulation time, 0.005 V step potential and voltage range from −0.25 V to +0.4 V.

The Electrochemical Impedance Spectroscopy (EIS) measurements were performed to provide more accurate information on the layer-by-layer reagent deposition on the sensing layer. The impedance measurements were performed at each stage over a wide frequency range (0.1 Hz and 0.1 MHz). The results were presented in the form of a Nyquist plot, with Randles' equivalent circuit ($R[Q(RW)]$) applied for data fitting.

All electrochemical experiments were performed in a three-electrode on-chip format at room temperature using a computer-controlled potentiostat Autolab PGSTAT101 (Metrohm). An electroactive substance, 10 mM PBS pH 7.4 containing 0.1 M KCl and 0.5 mM [Fe(CN)$_6$]$^{3-/4-}$ was used as the electrolyte solution for the electrochemical readings. All assays were run using the NOVA software, ver. 2.1.5 (Metrohm). The acquired data were evaluated using R Studio ver. 2022.12.0 + 353 (Posit PBC) and Prism 10 (GraphPad).

2.3. Biosensor fabrication

Based on the results obtained previously by our group, the following protocol was developed.

1. Cleaning the screen-printed substrates with Isopropyl Alcohol/Milli-Q water.

2. Characterization of bare screen-printed gold electrodes.

3. Immobilization of the linker at room temperature (RT) in dark.

4. Immobilization of the antibody at 37 °C.

5. Surface passivation with a blocking agent at 37 °C.

The incubation steps were all performed in a humidity-controlled condition. The electrodes were rinsed with a PBS solution (10 mM pH 7.4) and dried using pure nitrogen (N_2) stream after each modification steps. After the passivation step, the electrodes were rinsed with PBS Tween-20 solution and then PBS.

The next phase was to optimize the layer-by-layer deposition steps to enhance the chemical stability of the sensor as well as the sensor performance (Fig. 1). This was performed through optimizing the concentration and the incubation time of the linker, the antibodies, and the blocking agent, accordingly.

This was performed in various steps. First, several types of commercial and custom-made linkers, namely SH-PEG-NHS (abx085053) from Abexa, poly(2-ethyl-2-oxazoline) (PEtOx) polymer fabricated in-house[28] along with Sulfo-Lc-SDPD, 11-Mercaptoundecanoic acid (11-MUA), 3-Mercaptopropionic acid (MPA), dithiol, and ODT from Sigma-Aldrich, with different concentrations and various incubation times were compared. In this regard, various concentrations of each linker based on the incubation times mentioned in the literature or previous experiences of the research group were studied. The details of these experiments are explained elsewhere.[29]

The next step was to study the optimal antibody density on the surface to achieve the best immunosensor performance. In this regard, various concentrations of the antibody using different incubation times (2 h and overnight) were applied, while using the linker of choice as determined in the previous step. Thereafter, the calibration curves were plotted for each condition and the performance of the sensors was assessed.

The last step was to find the best material to suppress non-specific binding. The low and high-molecular weight blocking agents such as polyethylene glycol (PEG, MW $\approx$ 1 kDa), bovine serum albumin (BSA), ethanolamine (ETA), skim milk, and casein were compared. Different concentrations of these agents were tested. The surfactant Tween 20 was applied additionally in some conditions. The details of these experiments are explained elsewhere.[30]

The final multiplex immunosensor was aimed to be capable of working with both plasma and whole blood (WB) samples. For this purpose, a cartridge was designed by IMM Fraunhofer, Germany and fabricated by TE Connectivity, Spain (in the context of PoCOsteo) to house the microfluid manifold and the blisters containing the liquids needed for sample dilution, washing and measurement and facilitate the fluid flow from the capillary tube on the chip as the inlet to the reaction chamber for final readings. The cartridges were all vacuum packaged within 2 h of the preparation of the electrode array based on the protocol previously developed by our group.[31] The performance of the combined immunosensor (referred to as "OsteoLab" in the rest of the article) was therefore compared outside and inside this microsystem.

In the final step, the cartridges were tested using the point of care (PoC) tool developed by Labman Automation, UK (in the context of PoCOsteo) for the very purpose.

2.4. OsteoLab calibration

OsteoLab calibration was performed at two stages using the as-fabricated OsteoLab outside the microsystem, and later on in the system when OsteoLab was integrated into the above-mentioned PMMA cartridge. As for these tests, the sensors were incubated with known concentrations of the target analytes (BTM antigens). The OsteoLab operates based on a label-free detection strategy, relying on the progressive decrease of the redox probe ($[Fe(CN)_6]^{3-/4-}$) flux to the electrode surface due to the formation of the immunocomplex between the target analyte and the antibodies immobilized on the sensing layer of the electrode acting as a physical barrier. As a result, a decreased current reading is expected following the introduction of the higher concentrations of the analyte. The recovery index, calculated as the ratio of the current values read in the absence of the analyte ($C_{Target Analyte} = 0$) and in the presence of different concentrations of the target analyte ($C_{Target Analyte} = 100, 200, 400, 600, 800, 1000$ ng L^{-1} for CTx and 20, 40, 60, 80, 100 μg L^{-1} for PINP), were used to plot the calibration curves. In this step, the reaction time for the analyte to sufficiently react with the surface and achieve the best performance was optimized. This reaction time was, later on, used as the optimum time for plotting all the calibration curves and the tests using real samples. A four-parameter logistic (4 PL) curve fit was used to translate signal intensity to analyte concentration. This method is shown to "generate a 95% confidence interval of the limit of detection (LoD) estimate to provide a measure of uncertainty and a means by which to compare the analytical sensitivities of different assays statistically."[32]
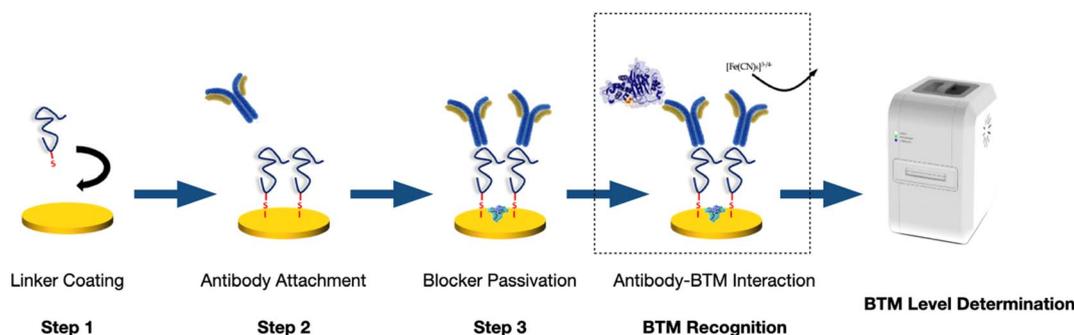

Fig. 1 A schematic illustration of the multistep surface functionalization of the as-fabricated label-free immunosensor for bone turnover maker detection. The tool shown as the last step for BTM level determination is a picture of the final PoC tool developed by Labman in the context of PoCOsteo for the same purpose. The validation of this tool is discussed further in this article.

The calibration curves were used to determine the LoD (=3.3(standard deviation of the response/slope of the calibration curve)), limit of quantification (LoQ = 10(standard deviation of the response/slope of the calibration curve)), sensitivity (slope of the calibration curve), and dynamic range of the immunosensors.[33,34] Based on the results, the inter- and intra-assay coefficients of variation (CV) were also assessed. The intra-assay CV is an average value calculated from the individual CVs (standard deviation (SD)/mean) for all of the duplicates. The inter-assay CV, on the other hand, is an expression of consistency and therefore, is calculated from the mean values for the high and low duplicate concentrations.

The reproducibility of the bare immunosensor was calculated using Residual Standard Deviation $\left(\text{RSD}_{\text{R}} = \dfrac{\text{standard deviation current}}{\text{average current}} \times 100\right)$ Horwitz ratio (HorRat) was used to assess the precision to be expected of the newly developed cartridge as a function of the concentration of the analyte:[35]

$$\text{HorRat} = \frac{\text{RSD}_{\text{R}}}{\text{PRSD}_{\text{R}}}$$

Predicted relative standard deviation (PRSD_{R}) was calculated using $2C^{-0.15}$, where C was the added concentration added, expressed as a mass fraction. The selectivity of the OsteoLab was tested by studying its cross-reactivity against 600 ng L^{-1} osteocalcin (Oc) and 600 ng L^{-1} PINP for the CTx immunosensor (CTx: 600 ng L^{-1}), and 60 μg L^{-1} Oc and 60 μg L^{-1} CTx for the PINP immunosensor (PINP: 60 μg L^{-1}) and PBS as the control in both immunosensors.

2.5. Laboratory validation

For the laboratory validation, two types of biofluids were used: Plasma and WB:

1. Plasma

First, the plasma separation was performed off-chip, simply through centrifuge as commonly performed in the central labs or using commercial anti-coagulant vacutainers (BD Life Sciences, Belgium). Different anticoagulants, currently available in the market, were tested and compared.

Their results were then compared with two plasma generator chips (A commercially available plasma generation chips developed by microfluidic ChipShop, Germany and one developed in-house by Fraunhofer IMM, Germany), with the aim integrating the best option in the final microfluidic manifold. Both chips used membranes with specific pore size to separate the plasma from whole blood. They were used as instructed by the developer.

The plasma generated using the above-mentioned techniques was later on tested using OsteoLab and the measured BTM levels were compared, with the results of the centrifuged samples used as gold-standard. The blood samples used for these tests were taken from healthy volunteers.

The next step was to determine the optimum dilution ratio. In this regard, serial dilution ratios of spiked samples (CTx: 200 ng L^{-1} and PINP: 10 μg L^{-1}) were compared to define the concentration within the working range that could provide a reliable result without affecting the performance of the immunosensor.

2. WB

WB samples were taken through finger pricks from healthy volunteers. As the first step, they were exposed in a commercially available capillary tube coated with the anti-coagulant of choice for different times, in order to determine the sufficient timing to prevent possible coagulation in the microfluidic channels later on in the study. The samples were then injected in a chip developed by Fraunhofer IMM, Germany, resembling the microfluidic structure of the final cartridge. The samples were incubated in the chip for 30 minutes, which was longer than the time needed for the sample to travel through the cartridge later on in the final device.

The samples were tested using the same procedure explained earlier in the plasma section to determine the optimum dilution ratio.

2.6. Clinical application

For Clinical application studies, the OsteoLab was incubated with samples (plasma and whole blood) from real patients. For the plasma studies, 20 samples already stored in the biobank of the Medical University of Graz (MUG) were used. The collection of these samples was conducted according to the World Medical Association Declaration of Helsinki and approved by the Ethical Committee of the Medical University Graz (20-492 ex 08/09). These samples were collected based on the common practice in the lab using Ethylenediaminetetraacetic acid (EDTA) as the anticoagulant. In order to compensate for the EDTA effects, they were treated with 1 M Calcium Chloride (CaCl$_2$) for two hours in +4 °C before being cast on the electrode array and incubated for 15 min (a protocol commonly used for similar purpose in ELISA tests).[36]

For WB studies, seven freshly collected finger prick samples from healthy volunteers with known BTM levels were used. After being exposed to Li–heparin for 2 min in the capillary tube, they were diluted (1 : 4 using PBS) and incubated on the OsteoLab for 15 min. The analyte concentration in each sample was then extrapolated based on the current read using the OsteoLab.

The plasma levels of CTx and PINP were tested in all samples (from the biobank or volunteers) using ECLIA (Elecsys 2010 autoanalyzer, Roche Diagnostics GmbH, Mannheim, Germany), as the state of the art. The Elecsys serum assay has an intra- and inter-assay CV of 2.7–4.1% and 1.7–6.5% for PINP and CTx, respectively. The results of ECLIA and OsteoLab were then compared, and a Bland–Altman graph was plotted to illustrate the agreement between these two readings for each marker.

When testing the PoC tool, several fresh finger prick samples from healthy volunteers were collected and transferred to the cartridge using the capillary tube placed on the cartridge to assess the feasibility of the tool to be used in practice for this purpose. The capillary tube was coated with the anticoagulant of choice based on the previous steps. The system automation was designed in a way that blood would remain in the tube for a specific time (equal to the optimum exposure time for anti-

coagulant as determined in the previous steps). This step also aims to confirm the system works properly as a whole.

3.   Results and discussion

3.1.   OsteoLab performance

A biosensor is created on a solid electrode surface by chemically or electrostatically attaching bio(macro)molecules such as proteins and nucleic acids. The first step in our research, therefore, was to define such surface. In brief, having the final objectives of the project, commercialization, in mind, an optimized protocol to screen print electrode arrays using high temperature gold ink on ceramic substrates was adopted (Fig. 2). The electrode arrays, produced by C-MAC using this protocol, were shown to be robust, repeatable and reproducible. The obtained current intensity of more than 30 arrays showed a mean of 2.3×10^{-7} A. Moreover, a simple cleaning step consisted of washing with isopropyl alcohol (IPA) and water with no additional pretreatment step was shown sufficient.

The dynamic range of an immunosensor and its sensing abilities is determined by the maximum loading capacity of its sensing layer. Therefore, the next step was to optimize the layer-by-layer deposition on the electrode surface. Maintaining the correct orientation, unperturbed conformation, and adequate density of the antibodies at the electrode surface is therefore critical to guarantee the array to be reproducible, biocompatible, cost-effective, with long-term stability and large surface area.[37] The comparison of several types of commercial and custom-made linkers with different concentrations and various incubation times revealed overnight immersion of the electrode substrates in a 10 mM ODT solution in ethanol as the linker of choice. Fig. 3 compares the calibration curve plotted for ODT and SH-PEG-NHS (one of the tested linkers). ODT, an alkanethiol with a long carbon chain, is mainly used as a self-assembled monolayer (SAM) for surface modification. It helps facilitate superhydrophobicity and reduce surface energy. The thiol groups were anchored on the gold surface, forming strong gold–sulphur bonds. Moreover, it also increases the CH_3 surface chemistry, which increases the antibody adsorption rate. The selective antigen recognition using this combination confirms the appropriate orientation of the antibody on the surface.

It is well-known that the selectivity of an immunosensor depends on not only the binding properties of the antibody but also the composition and the matrix of the target solution.[38] The
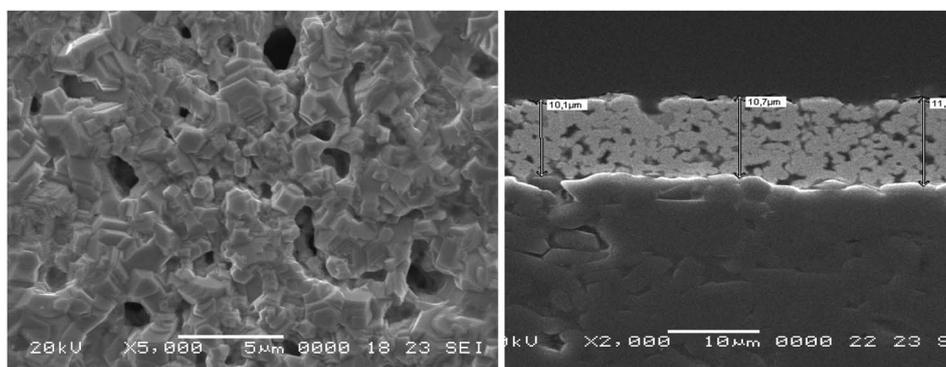

Fig. 2   SEM images of the C-MAC screen printed electrodes, with gold as the working electrode, used as the substrate throughout this study.
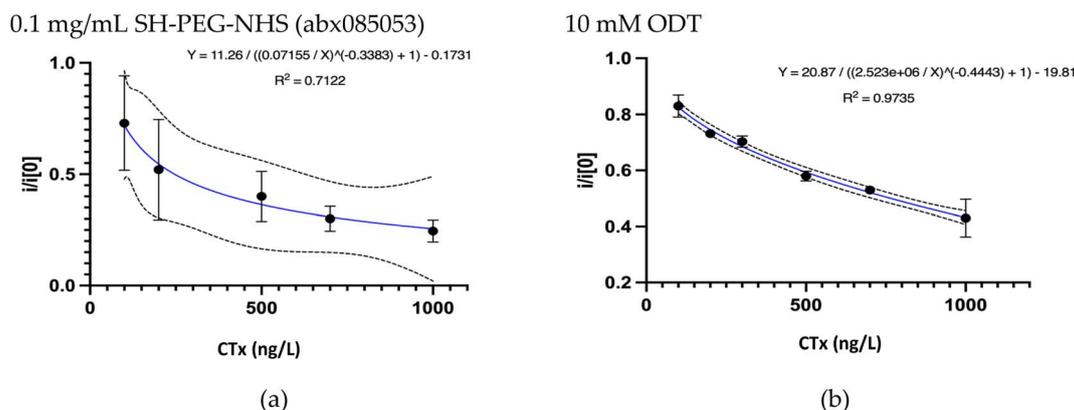

0.1 mg/mL SH-PEG-NHS (abx085053)

$Y = 11.26 / ((0.07155 / X)^{\wedge}(-0.3383) + 1) - 0.1731$
$R^2 = 0.7122$

10 mM ODT

$Y = 20.87 / ((2.523e+06 / X)^{\wedge}(-0.4443) + 1) - 19.81$
$R^2 = 0.9735$

(a)   (b)

Fig. 3   Calibration curve of the CTx immunosensor fabricated with (a) 0.1 mg mL^{-1} SH-PEG-NHS (abx085053) and (b) 10 mM ODT as the linker (the latter represents the performance of the final CTx immunosensor outside the microsystem). In both immunosensors various concentrations of CTx Antigen were used as the target analyte. 10 mM PBS pH 7.4 containing 0.1 M KCl and 0.5 mM $[Fe(CN)_6]^{3-/4-}$ was used as the electrolyte solution for the electrochemical readings. Calibration curve fitting is done using the 4 PL method.

assay interference, therefore, can result from the presence of cross-reacting species altering the concentration of the analytes in the sample or the antibody binding capacities. Both of which can lead to the misinterpretation of the results.

The use of monoclonal antibodies is shown to help improve the performance of the sensor by reducing the cross-reactivity towards other analytes commonly found in the blood/serum/plasma matrix. These endogenous molecules might have a similar structure or common cross-reactive epitopes with the target analyte. In this regard, custom-made monoclonal antibodies were designed by Proteogenix to only react with the target analyte and none of the known confounders (mentioned in the literature and the data sheet of the commercial kits). These results were confirmed in the preliminary ELISA tests.

In the next step, the concentration of the antibody was optimized. It is well-known that the density of the antibody on the electrode surface can significantly affect the immunosensor performance.[39] This is due to the fact that this factor can affect the surface conformation, thus the measured electrochemical signal, and finally the LoD and sensitivity of the immunosensor. Higher concentration of antibodies are shown to arrange differently on the surface and at the same time improve the antigen accumulation through increasing the solution resistance. Our results, similarly, showed higher antibody concentrations to be associated with better sensor performance. It was, therefore, concluded that using 100 μg mL^{-1} of each antibody (in PBS as the buffer) was associated with the highest linearity and sensitivity (Fig. 4). It was also shown that overnight incubation of the antibodies led to similar results as that of 2 h incubation. As a result, the latter was considered as the optimum incubation time throughout the study.

Apart from the application of monoclonal antibodies, in most studies, an additional blocking agent is applied to suppress nonspecific binding of the interfering substances more effectively. While many believe smaller and more hydrophilic molecules (such as ETA in our case) to have better blocking capacities, our studies showed casein 1% as the blocking agent of choice. As it could be seen in Fig. 5, the as fabricated immunosensors only react with the corresponding protein, confirming high specificity of these immunosensors. This also shows the optimum blocking agent should be chosen based on the molecular size of the

recognition element and that of the potential unwanted interferences.[40] Our results also corroborated with previous studies showing the improved capacity of milk phosphoprotein for preventing nonspecific binding in the presence of Tween 20, a known nonionic detergent.[41] For this reason, an additional washing step with PBS Tween 20 was considered as the final step. The final protocol is illustrated in the ESI.†

As mentioned earlier, the EIS was used to evaluate the layer-by-layer deposition and response to different concentrations of the analyte. As expected, the capacitive currents increased after casting each layer, demonstrating a significant change in the interfacial charge-transfer resistance (R_{ct}) and thus confirming the successful construction of the immunosensor (Fig. 6).

Next step was to plot the calibration curves using the known concentrations of the corresponding BTMs. The resulted DPV current intensities suggested the as-fabricated arrays to be fairly reproducible. As expected, compared with the freshly prepared arrays, a gradual decrease was registered in the DPV current peaks with any increase in the concentration of the target analytes (CTx: Fig. 3 and PINP: Fig. 7). This indicated the successful reaction between the sensing layer and the analyte. Compared to the corresponding targets, incubation with PBS or non-corresponding target analyte resulted in little or no decrease (typically <5%) in the current ($P < 0.05$). As already shown in Fig. 4, the as fabricated OsteoLab was also shown to be selective and highly specific for the target analyte.

It was also shown that 10 min for CTx and 15 min for PINP was sufficient, permitting the analyte to react with the surface antibodies; as the final goal, however, was to use both markers in a multiplex manner, 15 min was considered as the optimum reaction time.

Based on these plots, the two immunosensors were shown to be capable of measuring the target analyte with high sensitivity and beyond the recommended reference range (CTx: 104–1028 ng L^{-1} and PINP: 16–96 μg L^{-1}, correspondingly).[42] Both immunosensors were reported to be reproducible (RSD$_R$ CTx = 0.2, PINP = 0.24). The calculated LoD and detection range were comparable with commercial ECLIA kits (Table 1). The performance of the two immunosensors based on HorRat was also less than 2, which is considered acceptable.
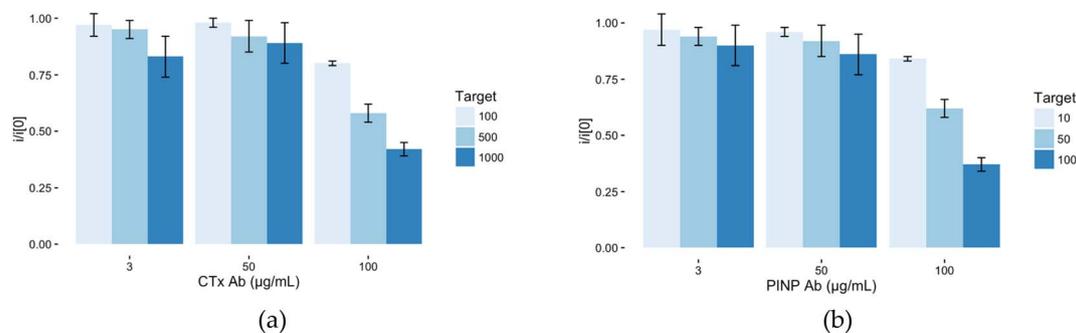

Fig. 4 Response of (a) CTx and (b) PINP immunosensors fabricated with various densities of the antibody selective to the corresponding target analyte in the step designed to determine the optimum antibody density. 10 mM PBS pH 7.4 containing 0.1 M KCl and 0.5 mM [Fe(CN)$_6$]$^{3-/4-}$ (1:1) was used as the electrolyte solution for the electrochemical readings.
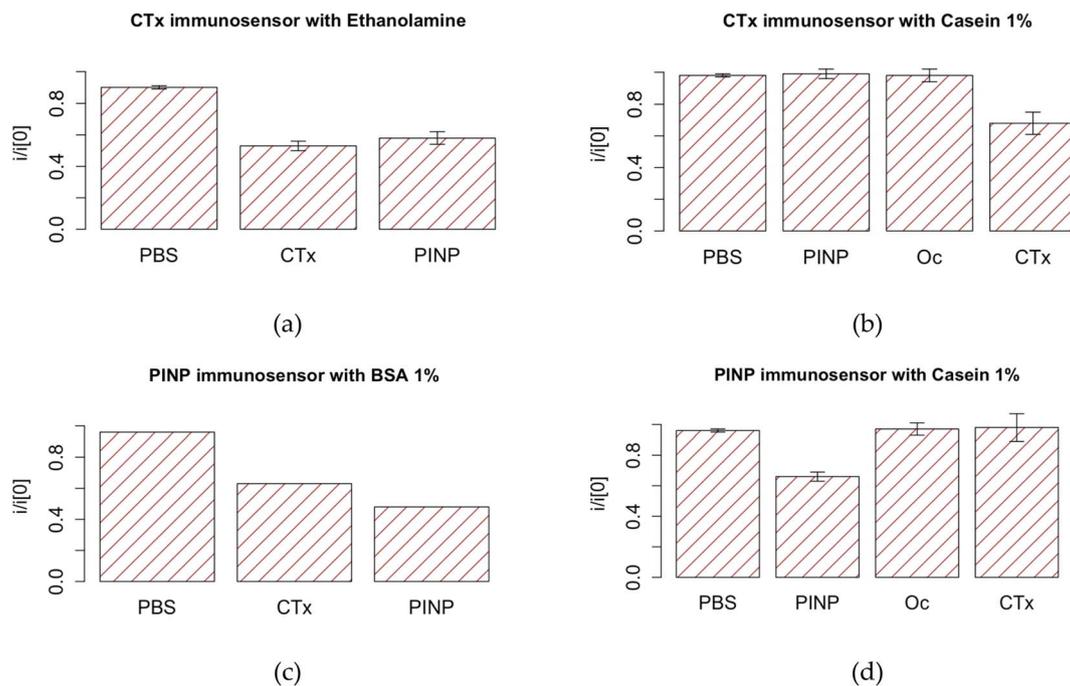
Fig. 5 Cross-reactivity tests of the (a, b) CTx (600 ng L^{-1} of Oc, PINP and CTx) and (c, d) PINP (60 μg L^{-1} of Oc, CTx and PINP) immunosensors fabricated using different blocking agents with other antigens and PBS as control. These tests were designed to determine the optimum blocking agent to improve the selectivity of the immunosensor. 10 mM PBS pH 7.4 containing 0.1 M KCl and 0.5 mM $[Fe(CN)_6]^{3-/4-}$ (1 : 1) was used as the electrolyte solution for the electrochemical readings.

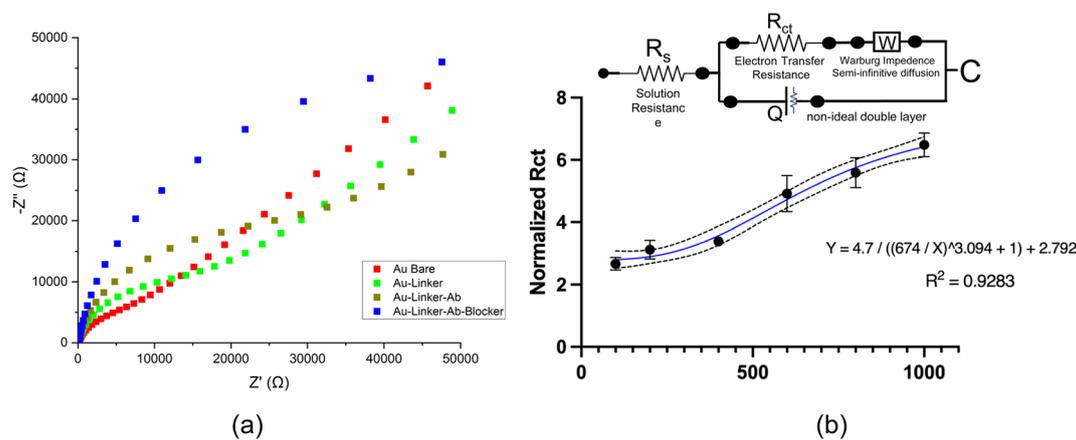**Fig. 6** Nyquist plots showing successful the layer-by-layer deposition on the sensing layer measurements performed at 0.2 V in $K_4[Fe(CN)_6]$/$K_3[Fe(CN)_6]$ over a frequency range of 0.1 Hz and 0.1 MHz. Inset: Randles'equivalent circuit ($R[Q(RW)]$) representing the sensing layer of the immunosensor. Calibration curve fitting is done using the 4 PL method.

Table 2 compares the characteristics of OsteoLab with some biosensors reported in the literature capable of measuring the IOF recommended biomarkers (CTx, PINP).

Most of the biosensors listed here were electrochemical biosensors; as compared to other technologies, such tools can offer higher sensitivity, lower detection limits, automation at reduced costs and miniaturization capabilities making them suitable for point of care applications. In comparison with existing optical biosensors, the main advantages of the electrochemical sensors include not requiring expensive infrastructure and having shorter turnaround time.[26,44] From among the electrochemical biosensors, the labeled and sandwich immunosensors are more expensive, making the label-free ones more appropriate for screening purposes.[18]

Apart from the multiplexing capacity (based on the IOF recommended biomarkers), the OsteoLab's broad dynamic range is another advantage over similar sensors reported in literature.[21] This is of great importance, because as for the CTx immunosensor the accurate measurement of higher concentrations for treatment monitoring and for PINP, on the other hand, the LoD of the sensor to identify at-risk individuals is of utmost importance.[5]
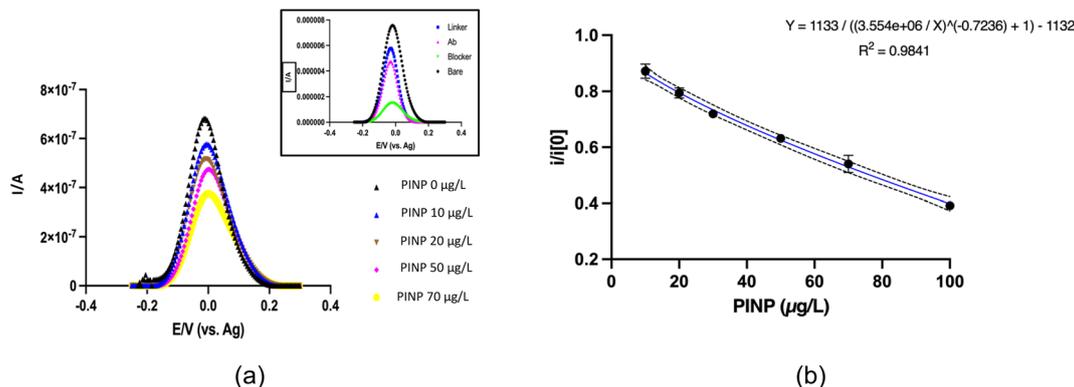
Fig. 7 (a) DPV readings of different concentrations of PINP as the target analyte and (b) calibration curve of the PINP immunosensor tested outside the microsystem housing. 10 mM PBS pH 7.4 containing 0.1 M KCl and 0.5 mM $[Fe(CN)_6]^{3-/4-}$ (1 : 1) was used as the electrolyte solution for the electrochemical readings. Calibration curve fitting was done using the 4 PL method.

Table 1 CTx and PINP sensor performance (outside microsystem)

Target protein	CTx (ng L^{-1})	PINP (µg L^{-1})
R^2	0.97	0.98
Detection range	50–1500	0.3–150
LoD	15	008
LoQ	49	0.28
CV (inter-assay)	5.39% (2.17–8.61)	6.81% (1.07–3)
CV (intra-assay)	6.97% (1.47–8.67)	5.37% (1.06–5.19)
RSD_R	0.2	0.24
HorRat[a]	0.65	0.84

[a] For 1 ng L^{-1} for CTx and 1 µg L^{-1} for PINP.

3.2. Laboratory validation of OsteoLab

OsteoLab was validated using real plasma and whole blood samples.

1. Plasma

First, the existing commercial anticoagulants were compared. Considering their mechanism of action, the outcome differed:

- Ethylenediaminetetraacetic acid (EDTA): the chelation effects of EDTA on the calcium (Ca)/thrombin levels negatively affected the sensor performance. However, the issue was resolved by adding Ca to the samples, as performed in certain ELISA measurements.[36,45]

- Citrate and sodium (Na)–heparin had negative effects on the sensor performance. The former reacted with the gold surface, producing gold citrate, whereas the main reason behind the effects of the latter is not clear.

- Lithium (Li)–heparin resulted in promising results, comparable with that of ELISA. It was therefore concluded as the anticoagulant of choice in the future steps.

In the next step, the ChipShop and IMM plasma generator chips were compared. Despite being significantly more efficient

Table 2 Characteristics of biosensors reported in the literature for measuring CTx or PINP (based on IOF guidelines)[a]

	Dynamic range	Marker	Technology/measurement
OsteoLab	50–1500	CTx (ng L^{-1})	Label-free immunosensor/DPV
	0.3–150	PINP (µg L^{-1})	
Ramanathan et al.[13]	50–600	CTx (ng L^{-1})	Gold-deposited CNT/EIS
Afsarimanesh et al.[14]	147–1693	CTx (ng L^{-1})	Label-free immunosensor/EIS
Yun et al.[16]	50 000–3 × 10^6	CTx (ng L^{-1})	Label-free immunosensor/EIS
Afsarimanesh et al.[43]	100–2500	CTx (ng L^{-1})	Molecular imprinting technology/EIS
Khashayar et al.[27]	9000–42 000	Oc (ng L^{-1})	Label-free immunosensor/DPV
	25–1008	CTx (ng L^{-1})	
Park et al.[44]	200–2800	Urinary CTx (ng $mmol^{-1}$)	Sandwich FMGC, microbead counting
	0–2500	Serum CTx (ng L^{-1})	
Han et al.[18]	2–64	PINP (µg L^{-1})	Sandwich immunosensor (amine-modified zeolite)/
Claudon et al.[26]	500–2.8 × 10^5	Oc (ng L^{-1})	Labeled immunoassay/CCD camera
	50–2000	CTx (ng L^{-1})	
	25–85	PINP (µg L^{-1})	
	0.05–2500	PTH (ng L^{-1})	

[a] EIS: electrochemical impedance spectroscopy, FMGC: fluoro-microbeads guiding chip; CCD: charge coupled device; CNT: carbon nanotube; EIS: electrochemical impedance spectroscopy; CTx: C-terminal telopeptide of type I collagen; PINP: Procollagen I Intact N-Terminal; PTH: parathyroid hormone; DPV: differential pulse voltammetry; Oc: osteocalcin.

compared to their counterparts (high yield of about 70%), the produced plasma using either chip was not sufficient to completely fill the microfluidic channels; as a result, dilution was inevitable. It should be noted that while dilution can negatively affect the LoD, it can improve the system accuracy through reducing the matrix effect. This is different from the dilution linearity test commonly performed in ELISA kits on samples with a concentration higher than the LoQ of the kit.[46] The results of the serial dilution studies revealed 1 : 10 (1 part plasma, 9-part PBS) dilution for CTx and 1 : 4 for PINP as the highest acceptable dilution ratios, not compromising the LoD of the immunosensors. As a result, 1 : 4 dilution ratio was considered optimum considering the multiplex testing.

2. Whole blood

Previous studies have shown the viscosity of WB, which is known to increase with aging, to vary between 5 and 120 mPa.[47] Using a chip resembling the microfluidic structure of the final cartridge, the coagulation risk of heparinized WB with various dilution factors was evaluated after a 30 min incubation period. Results revealed no clotting incidence in the 1 : 4 diluted heparinized WB samples as well as negligible effects on the LoD and LoQ of the OsteoLab using these samples. Again, 1 : 4 was considered as the optimum dilution ration for the WB samples.

3.3. Clinical application of OsteoLab

Subsequently, practical application of the immunosensors using the abovementioned protocols was evaluated using real plasma and WB samples.

Twenty biobank plasma samples, treated with EDTA at the time of collection, were used. After exposing them to 1 M $CaCl_2$ based on the abovementioned protocol, the samples were tested in OsteoLab. Fig. 8 shows high agreement between the readings of the as fabricated immunosensor and that of ECLIA. The black line in the correlation plot suggests the ideal situation where the two readings were the same. The further the dots are from the line suggests the larger difference between the two readings. As it could be seen in the figures, CTx readings of the two instruments have higher agreement and thus lower difference compared with that of PINP. Bland–Altman plots are used to assess the agreement of the new instrument compared with the state-of the art. The horizontal straight line in the middle of the chart shows the average difference in the measurements or the bias between the two instruments. Values further from zero suggest the larger bias in the new instrument. Fig. 9 shows a small average difference and a narrow confidence interval in the Bland–Altman plots, suggesting a low relative error in the OsteoLab measurements.
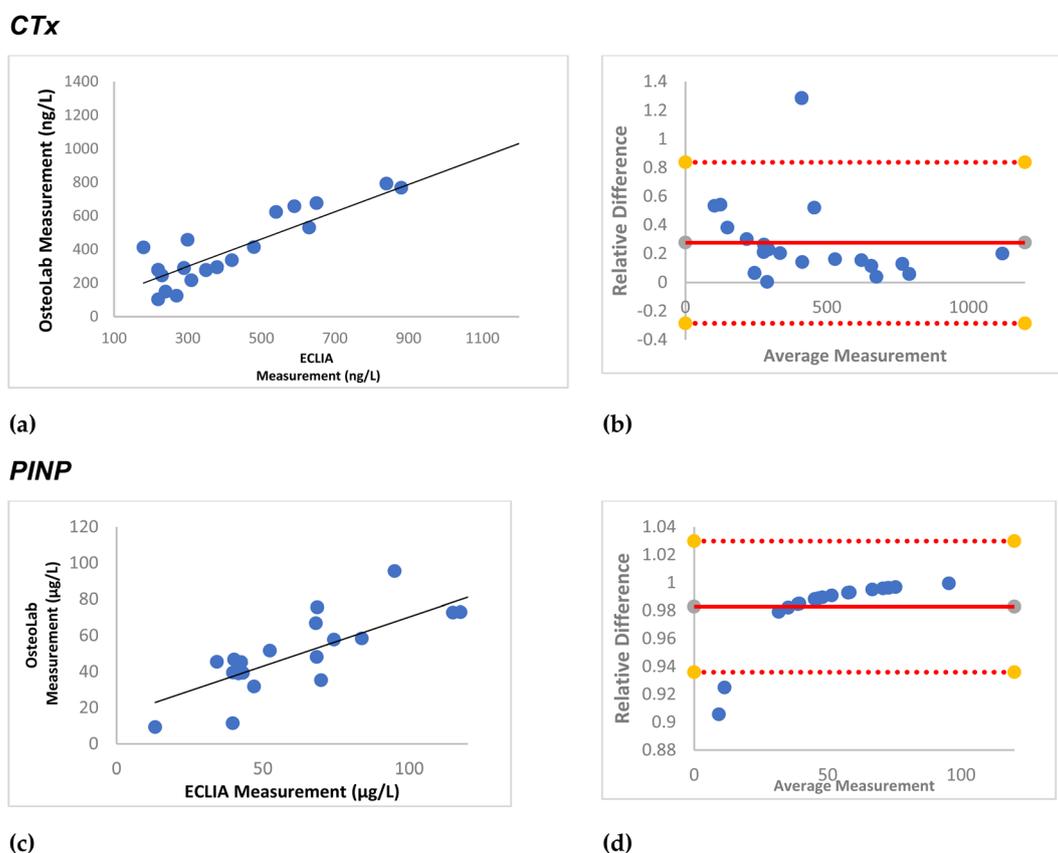
Fig. 8 Correlation (a, c) and Bland–Altman (b, d) plots for real serum/plasma samples tested using OsteoLab sensor and ECLIA as the state-of the art for each BTM. In the correlation plot, the 1 : 1 line is used as a reference to visualize the difference between the readings of the two instruments. In the Bland–Altman plot, the y axis shows the difference between the two paired measurements and the x axis illustrates the average values obtained with the 2 methods. The horizontal plain line represents the average difference between the 2 assays and the dotted lines the 95% CI.
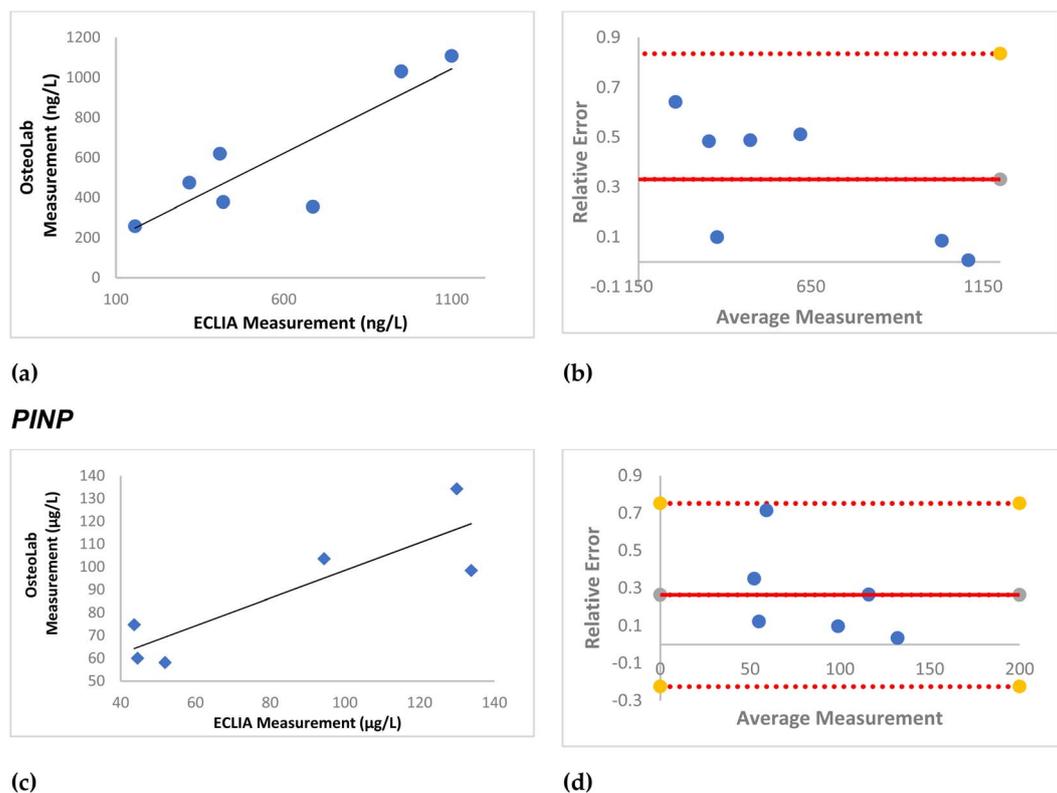
(a)

(b)

PINP

(c)

(d)

Fig. 9 Correlation (a, c) and Bland–Altman (b, d) plots for real whole blood samples tested using OsteoLab sensor and ECLIA as the state-of the art for each BTM. In the correlation plot, the 1 : 1 line is used as a reference to visualize the difference between the readings of the two instruments. In the Bland–Altman plot, the y axis shows the difference between the two paired measurements and the x axis illustrates the average values obtained with the 2 methods. The horizontal plain line represents the average difference between the 2 assays and the dotted lines the 95% CI.

These differences could be due to the effect of the $CaCl_2$ treatment step on the levels of the target analyte in the test samples.

In the next step, seven fresh finger prick samples were collected in Li–heparin coated capillary tubes. After 2 min, they were diluted (1 : 4 using PBS) and incubated on the OsteoLab for 15 min. Fig. 9 shows high agreement between the readings of the OsteoLab and ECLIA. The calculated errors in the Bland–Altman plots, however, were smaller than those of the plasma blood samples. The lower number of samples in these tests, though, makes the comparison between the plasma and WB readings rather difficult.

3.4. Laboratory validation of the OsteoLab cartridges

As for the next step, the OsteoLab was placed in the cartridges housing the microfluidic manifolds and the required add-ons. Preliminary experiments had revealed that oxygen (O_2), humidity and light affect the performance of the immunosensor negatively. As a result, vacuum packaging using a multilayer sheet of Polyamide (PA)/Polyethylene (PE)/Ethylene vinyl alcohol (EVOH)/PE was selected as the packaging technique of choice to preserve the shelf-life of the sensors. This multilayer is commercially used for the preservation of O_2-sensitive food products. The packaged immunosensors were shown to survive

at least 10 months of storage at room temperature with negligible changes in their performance. The detailed explanation of the stability, repeatability and reproducibility of these packaged immunosensors is published elsewhere.[31]

The vacuum-packed Osteolab cartridges were shown to be comparable with the freshly made immunosensors (Fig. 10).

Thereafter, the OsteoLab cartridge was tested using the first generation of the PoC Tool developed for the same purpose (Fig. 1). This tool contains a built-in potentiostat (LabStat) and the required electronic and Pneumatic systems for efficient fluidic flow and sample measurement. Unlike its commercially available counterparts, LabStat allows the working electrodes to be read simultaneously, reducing the measurement time (6–10 s vs. a couple of minutes) as well as enhancing the consistency and accuracy of the tests. The system is also scalable to read up to 64 working electrodes at the same time, making it suitable for more complex applications.

Fresh finger prick samples were collected using the built-in capillary tube in the cartridge, which was inserted in the PoC tool and tested. The preliminary results revealed successful performance of tasks such as sample preparation, fluidic flow and assessment of the results. The BTM readings were also comparable with that of ECLIA. Further tests however are needed to finalize the tool validation steps.
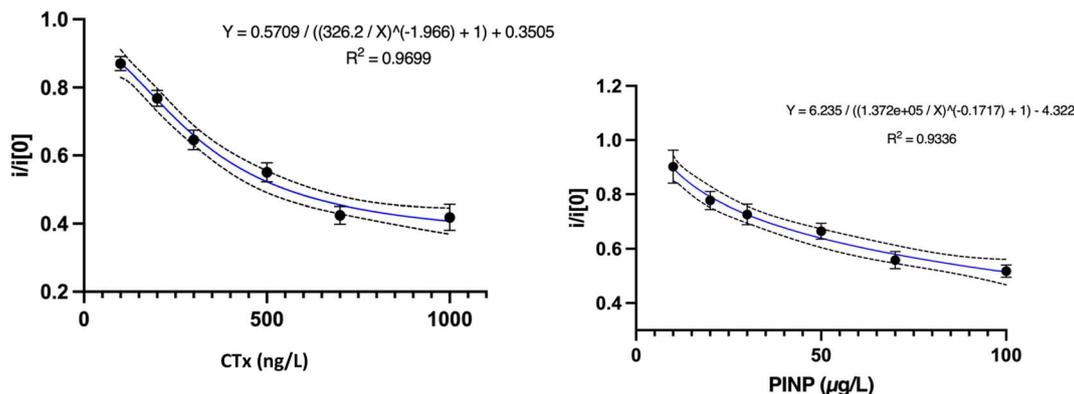
Fig. 10 Calibration curve of CTx and PINP immunosensors inside the microsystem housing. 10 mM PBS pH 7.4 containing 0.1 M KCl and 0.5 mM $[Fe(CN)_6]^{3-/4-}$ (1 : 1) was used as the electrolyte solution for the electrochemical readings. Calibration curve fitting was done using the 4 PL method.

4. Conclusions

The goal of this study was to develop a sensitive, reliable, portable, and cost-effective platform for the measurement of BTMs in real time. This is the first time such a multiplex platform for the measurement of BTMs in various biofluids (WB or plasma) with high sensitivity and selectivity has been developed.

The results showed high agreement with ECLIA, as the state-of-the-art, while providing a much shorter turnaround time of about 15 min. The proposed platform uses a sample volume of 10 µl, which is much lower than that needed by its counterparts including ELISA and ECLIA. At the same time, it reduces the amount of the reagents needed for each test to as low as only 2 µl for each marker.

The obtained data also confirmed the possibility of storing the as-fabricated vacuum-packed cartridges up to 10 months in RT, which has never been reported for similar immunosensors. Compared to the existing biosensors, OsteoLab has a broader dynamic range as well as the capability for multiplexing, turning it into a promising diagnostic tool for the assessment of bone loss and treatment monitoring. Further studies are needed to finalize the clinical validation of OsteoLab, showing its practicality for use in clinical practice. The idea is to test the same platform with other biological fluids such as saliva, urine, or sweat to provide a non-invasive analytical option. However, the accuracy and practicability of using BTM levels in such biofluids should be assessed first.

Institutional review board statement

The study is conducted according to the World Medical Association Declaration of Helsinki and approved by the Ethical Committee of the Medical University Graz (20-492 ex 08/09).

Informed consent statement

An informed consent was signed by all the patients.

Data availability

Available upon request.

Author contributions

Conceptualization, PK, HPD; methodology, PK, JV, PR, RH, DL, RG, DL, PB, IE and HPD; validation, BL, BOP, HPD, and PK; formal analysis, PK, PL, PR, RH, DL, RG, DL, PB, IE.; writing—original draft preparation, PK.; writing—review and editing, everyone; project administration, PK, JV.; funding acquisition, everyone. All authors have read and agreed to the published version of the manuscript.

Conflicts of interest

The authors declare no conflict of interest.

Acknowledgements

References

1 N. Salari, H. Ghasemi, L. Mohammadi, M. hasan Behzadi, E. Rabieenia, S. Shohaimi and M. Mohammadi, *J. Orthop. Surg. Res.*, 2021, **16**, 1–20.

2 J. T. Lin and J. M. Lane, *Clin. Orthop. Relat. Res.*, 2004, **425**, 126–134.

3 H. P. Dimai, *Bone*, 2017, **104**, 39–43.

4 J. Kanis, O. Johnell, A. Oden, C. De Laet, B. Jonsson and A. Dawson, *Bone*, 2002, **30**, 251–258.

5 P. Khashayar, H. Aghaei Meybodi, G. Amoabediny and B. Larijani, *Recent Pat. Endocr., Metab. Immune Drug Discovery*, 2015, **9**, 79–89.

6 P. M. Camacho, S. M. Petak, N. Binkley, B. L. Clarke, S. T. Harris, F. L. Daniel Hurley, M. Kleerekoper, E. Michael Lewiecki, P. D. Miller, H. S. Narula, R. Pessah-

Pollack, V. Tangpricha, S. J. Wimalawansa and N. B. Watts, *Endocr. Pract.*, 2016, DOI: 10.4158/EP161435.GL.

7 E. K. Sackmann, A. L. Fulton and D. J. Beebe, *Nature*, 2014, **507**, 181–189.

8 C. H. Wu, Y. F. Chang, C. H. Chen, E. M. Lewiecki, C. Wüster, I. Reid, K. S. Tsai, T. Matsumoto, L. B. Mercado-Asis, D. C. Chan, J. S. Hwang, C. L. Cheung, K. Saag, J. K. Lee, S. Te Tu, W. Xia, W. Yu, Y. S. Chung, P. Ebeling, A. Mithal, S. L. Ferrari, C. Cooper, G. T. Lin and R. Sen Yang, *J. Clin. Densitom.*, 2021, **24**(1), 3–13.

9 P. Hadji, N. Papaioannou, E. Gielen, M. Feudjo Tepie, E. Zhang, I. Frieling, P. Geusens, P. Makras, H. Resch, G. Möller, L. Kalouche-Khalil and A. Fahrleitner-Pammer, *Osteoporosis Int.*, 2015, **26**(10), 2479–2489.

10 M. Focke, D. Kosse, C. Muller, H. Reinecke, R. Zengerle and F. Von Stetten, *Lab Chip*, 2010, **10**, 1365–1386.

11 D. Sung, D. H. Shin and S. Jon, *Biosens. Bioelectron.*, 2011, **26**(9), 3967–3972, DOI: 10.1016/j.bios.2011.03.005.

12 C. I. Fernandez-Lazaro, J. M. García-González, D. P. Adams, D. Fernandez-Lazaro, J. Mielgo-Ayuso, A. Caballero-Garcia, F. Moreno Racionero, A. Córdova and J. A. Miron-Canelo, *BMC Fam. Pract.*, 2019, **20**, 1–12.

13 M. Ramanathan, M. Patil, R. Epur, Y. Yun, V. Shanov, M. Schulz, W. R. Heineman, M. K. Datta and P. N. Kumta, *Biosens. Bioelectron.*, 2016, **77**, 580–588.

14 N. Afsarimanesh, M. E. E. Alahi, S. C. Mukhopadhyay and M. Kruger, *J. Sens. Actuator Netw.*, 2018, **7**(1), 10.

15 N. Afsarimanesh, S. C. Mukhopadhyay and M. Kruger, in *Smart Sensors, Measurement and Instrumentation*, Springer International Publishing, 2019, vol. 30, pp. 45–57.

16 Y. H. Yun, A. Bhattacharya, N. B. Watts and M. J. Schulz, *Sensors*, 2009, **9**, 7957–7969.

17 L. Sappia, B. Felice, M. A. Sanchez, M. Martí, R. Madrid and I. Pividori, *Sens. Actuators, B*, 2019, **281**, 221–228.

18 X. Han, Z. Su, Q. Liu, S. C. B. Gopinath and J. Chen, *Mater. Express*, 2022, **12**, 1042–1048.

19 P. Khashayar, G. Amoabediny, M. Hosseini, R. Verplancke, F. Razi, J. Vanfleteren and B. Larijani, *IEEE Sens. J.*, 2017, **17**, 3367–3374.

20 Q. Chang, J. Huang, L. He, F. Xi, Y. Zhang, Z. Lu and Z. Yang, *Front. Chem.*, 2022, **10**, 940795.

21 P. Khashayar, G. Amoabediny, B. Larijani, M. Hosseini, R. Verplancke, D. Schaubroeck, S. Van Put, F. Razi, M. De Keersmaecker, A. Adriaens, *et al.* A Multiplexed Microfluidic Platform for Bone Marker Measurement: A Proof-of-Concept, *Micromachines*, 2017, **8**, 133.

22 S. Vasikaran, R. Eastell, O. Bruyère, A. J. Foldes, P. Garnero, A. Griesmacher, M. McClung, H. A. Morris, S. Silverman, T. Trenti, D. A. Wahl, C. Cooper and J. A. Kanis, *Osteoporosis Int.*, 2011, **22**, 391–420.

23 P. Szulc, K. Naylor, N. R. Hoyle, R. Eastell and E. T. Leary, *Osteoporosis Int.*, 2017, **28**, 2541–2556.

24 MayoClinic Laboratories, *CTX Beta-CrossLaps (Beta*CTx), Serum: Clinical & Interpretive*, 2023, https://www.mayomedicallaboratories.com/test-catalog/Clinical+and+Interpretive/83175.

25 Mayoclinic Laboratories, *PINP - Overview: Procollagen I Intact N-Terminal, Serum: Clinical & Interpretive*, https://www.mayocliniclabs.com/test-catalog/overview/61695#Clinical-and-Interpretive, accessed 3 December 2023.

26 A. Claudon, P. Vergnaud, C. Valverde, A. Mayr, U. Klause and P. Garnero, *Clin. Chem.*, 2008, **54**, 1554–1563.

27 P. Khashayar, G. Amoabediny, B. Larijani, M. Hosseini, R. Verplancke, D. Schaubroeck, S. Van Put, F. Razi, M. De Keersmaecker, A. Adriaens, S. Goemaere and T. Fiers, *Micromachines*, 2017, **8**, 133.

28 O. Sedlacek, T. Egghe, P. Khashayar, M. Purino, P. Lopes, J. Vanfleteren, N. De Geyter and R. Hoogenboom, *Bioconjugate Chem.*, 2023, **34**(12), 2311–2318.

29 P. Khashayar, *et al.*, Under Rev.

30 P. Khashayar, *et al.*, Under Rev.

31 A. Vermeulen, P. Lopes, F. Devlieghere, P. Ragaert, J. Vanfleteren and P. Khashayar, *IEEE Sens. J.*, 2024, **24**(8), 13122–13128.

32 C. A. Holstein, M. Griffin, J. Hong and P. D. Sampson, *Anal. Chem.*, 2015, **87**, 9795–9801.

33 G. W. J. Latimer, *Official Methods of Analysis of AOAC International*, AOAC Publications, New York, 2023.

34 *Q2(R1) Validation of Analytical Procedures: Text and Methodology Guidance for Industry*, Rockville, 2017.

35 W. Horwitz and R. Albert, *J. AOAC Int.*, 2006, **89**, 1095–1109.

36 E. Tenland and M. Hillman, *Clin. Chem. Lab. Med.*, 2013, **51**, e145–e147.

37 N. G. Welch, J. A. Scoble, B. W. Muir and P. J. Pigram, *Biointerphases*, 2017, **12**, 02D301.

38 J. Tate and G. Ward, *Clin. Biochem. Rev.*, 2004, **25**, 105.

39 J. Zorea, R. P. Shukla, M. Elkabets and H. Ben-Yoav, *Anal. Bioanal. Chem.*, 2020, **412**, 1709.

40 M. V. Riquelme, H. Zhao, V. Srinivasaraghavan, A. Pruden, P. Vikesland and M. Agah, *Sens. Bio-Sens. Res.*, 2016, **8**, 47–54.

41 M. Steinitz, *Anal. Biochem.*, 2000, **282**, 232–238.

42 P. D. Delmas, P. Eastell, P. Garnero, M. J. Seibel and J. Stepan, for the Committee of Scientific Advisors of the International Osteoporosis Foundation, *Osteoporosis Int.*, 2000, **11**, S2–S17.

43 N. Afsarimanesh, S. C. Mukhopadhyay and M. Kruger, *IEEE Trans. Biomed. Eng.*, 2018, **65**, 1264–1271.

44 Y. M. Park, S. J. Kim, K. J. Lee, S. S. Yang, B.-H. Min and H. C. Yoon, *Biosens. Bioelectron.*, 2015, **67**, 192–199.

45 E. Nilson, B. Ekholm, B. Rees Smith, C. Törn and M. Hillman, *Clin. Chim. Acta*, 2008, **388**, 130–134.

46 U. Andreasson, A. Perret-Liaudet, L. J. C. van Waalwijk van Doorn, K. Blennow, D. Chiasserini, S. Engelborghs, T. Fladby, S. Genc, N. Kruse, H. B. Kuiperij, L. Kulic, P. Lewczuk, B. Mollenhauer, B. Mroczko, L. Parnetti, E. Vanmechelen, M. M. Verbeek, B. Winblad, H. Zetterberg, M. Koel-Simmelink and C. E. Teunissen, *Front. Neurol.*, 2015, **6**, 179.

47 M. J. Simmonds, H. J. Meiselman and O. K. Baskurt, *J. Geriatr. Cardiol.*, 2013, **10**, 291–301.